Positional Effects of Annelated Pyrazine Rings on Structure and Stability of Hydrogen-bonded Frameworks of Hexaazatrinaphthylene Derivatives

Ichiro Hisaki,[†,§,#,*] *Qin Ji,*[§] *Kiyonori Takahashi,*[†,§] *Norimitsu Tohnai,*[‡] *Takayoshi Nakamura*[†,§]

[†] Research Institute for Electronic Science, Hokkaido University, N20W10 Sapporo, Hokkaido 001-0020, Japan

[§] Graduate School of Environmental Science, Hokkaido University, N10W5 Sapporo, Hokkaido 060-0810, Japan

[‡] Department of Material and Life Science, Graduate School of Engineering, Osaka University, 2-1 Yamadaoka, Suita, Osaka 565-0871, Japan.

[#] Present address: Graduate School of Engineering Science, Osaka University, 1-3 Machikaneyama, Toyonaka, Osaka 560-8531, Japan. Email: hisaki@chem.es.osaka-u.ac.jp

Key words: Porous framework, hydrogen-bond, quinoxaline, hexaazatrinaphthylene, acid responsiveness

ABSTRACT A porous hydrogen-bonded organic framework (HOF) composed of N-hetero π-conjugated molecules (Nπ-HOF) is a promising candidate for multi-functional porous materials. However, such HOFs are still limited and only handful examples were reported. In this study, we investigated positional effects of annelated pyrazine-rings on structure and stability of Nπ-HOFs

to establish design principle of Nπ-HOFs. A new isomer of hexaazatrinaphthylene (**CPBTQ**) was synthesized and subjected to Nπ-HOF construction, activation, evaluation of stability and permanent porosity. Comparison between two kinds of Nπ-HOF composed of isomers (**CPBTQ** and **CPHATN**) possessing three pyrazine rings annelated at the different positions indicates that the positional difference of the pyrazine rings strongly effects on conformation of the peripheral phenylene groups, which then lead to different structure and stability of the Nπ-HOFs. The Nπ-HOF composed of **CPBTQ (CPBTQ-1a)** are revealed to exhibit the Brunauer-Emmett-Teller surface area of 471 m^2g^{-1} and show HCl responsiveness thanks to the basic pyrazine rings annelated to the triphenylene core. We believe that the present results can contribute not only for construction of multifunctional porous materials but also for chemistry on hetero-aromatic compounds.

Introduction

Nitrogen (N)-containing relatives of polycyclic aromatic hydrocarbons (aza-PAHs) have recently attracted much attention regarding application for organic semiconducting materials, sensors, and so on. These include linear azaacenes,[1–4] star-shaped azatriphenylene,[5] discotic azabenzocoronene,[6,7] and bowl-shaped aza-PAHs[8] such as azacorannulene[9] and azasumanene.[10] Incorporation of N atoms into the π-conjugated systems is capable of fine-tuning electronic states of the systems,[11–14] capturing and sensing cationic species,[15,16] making metal complexes,[17–21] and improving molecular packing in crystalline states through C–H···N interactions[22] or dative bonds[23] to achieve effective charge-transport properties. To date, systematic studies on relationship among numbers and positions of the N atoms in the system, molecular properties, aggregate structures, and solid state properties were conducted from theoretical and experimental aspects. Bunz, Dreuw, Himmel, and co-workers reported spectroscopic precise analyses of tetracene analogues with different numbers of N atoms in solid noble-gas matrices.[24] Day and co-workers reported organic semiconduction properties of pentacene analogues with 5 or 7 N atoms based on the predicted crystal structures, energy evaluation, and calculated charge carrier mobility.[25] Theoretical calculation on reorganization energies were also reported.[26] Isoda, Tadokoro, and co-workers demonstrated redox properties of azaacene-based in liquid crystalline states.[27] Bonifazi and co-workers conducted systematic crystallization of aza-PAHs and boronic acids via hydrogen-bonding to yield various co-crystals.[28] However, effects of N atoms in aza-PAHs on their molecular arrangements in hydrogen-bonded organic frameworks (HOFs) with permanent porosity have not fully been understood.

HOFs are porous molecular crystal particularly constructed through intermolecular hydrogen bonds. Because of their high crystallinity, easy recrystallization process to obtain, and

developing design strategy based on multiplicity and/or directionality of hydrogen bonds, various HOFs have been constructed and investigated their properties as a new class of porous frameworks.[29–35] In connection with HOFs, we previously demonstrated that C_3-symmetric π-conjugated hydrocarbons, such as a triphenylene derivative **Tp**, possessing six carboxyphenyl groups in their periphery (Chart 1) form hydrogen-bonded hexagonal network (H-HexNet) and that the H-HexNet stacks without interpenetration to yield the corresponding layered HOFs.[36–38] More recently, Chen and coworkers report a HOF based on C_3- or C_6-symmetric benzene derivatives with carboxy groups.[39,40] Interestingly, when the triphenylene moiety of **Tp** was replaced by hexaazatriphenylene (HAT), the resulting derivative **CPHAT** formed no layered 2D framework but a three-dimensional (3D) rigid framework with permanent porosity.[41,42] In the 3D framework, the HAT moiety is deformed into a propeller-shaped conformation by packing forces. Because of the conformation, the six peripheral carboxyphenyl groups alternately direct upward and downward to form a 3D H-bonded network. These results are crucially provided by introduction of pyrazine rings into the π-conjugated core. Subsequently, we synthesized its larger analogue, carboxyphenyl-substituted hexaazatrinaphthylene derivative (**CPHATN**).[43] **CPHATN** was revealed to form a very stable porous layered framework based on the 2D H-HexNet. Importantly, the framework is responsive to HCl vapor or solution by changing its color from yellow to brown due to protonation of the pyrazine rings.

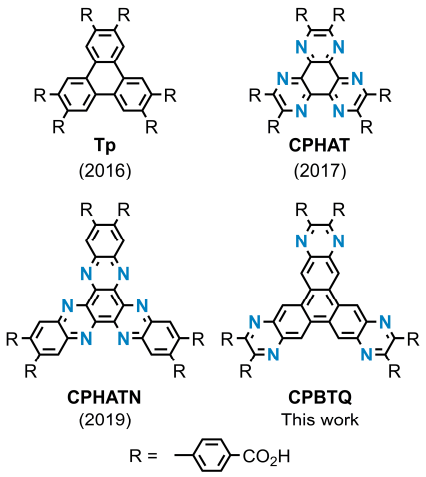

Chart 1. *C*$_3$-symmetric π-conjugated molecules (C_3PI) without and with incorporated pyrazine rings as a building blocks to construct porous hydrogen-bonded organic frameworks.

Keeping this in mind, we became interested in a H-bonded assembly structure of carboxyphenyl-substituted benzotriquinoxaline derivative **CPBTQ**. **CPBTQ** possess three pyrazine rings annelated in different position from **CPHATN**. Therefore, comparison of the assembly structures of these two regioisomers can provide a positional effects of the N-hetero-rings on molecular arrangements and properties.

In this paper, synthesis and characterization of **CPBTQ**, construction and structural determination of its HOF, evaluation of porosity and stability of the activated HOF, acid responsiveness, and effects of the N atoms in **CPBTQ** on structure and property of the HOF are described. Interestingly, **CPBTQ** forms a H-HexNet-based HOF with the different stacking manner of H-HexNet sheets from that of **CPHATN**. The H-HexNet involves desociated and pertly H-bonded dimers, in addition to fully H-bonded carboxy dimer (Figure 1). Moreover, it is revealed that the position of the pyrazine rings strongly effects on conformation of the peripheral phenylene groups, which then makes the structure, particularly H-bonding patterns, and property

of the HOF different from that of **CPHATN**. We believe that the present results can contribute not only for construction of new functional N-hetero π-conjugated molecule-based HOFs (Nπ-HOFs), but also for chemistry on hetero-aromatic compounds.

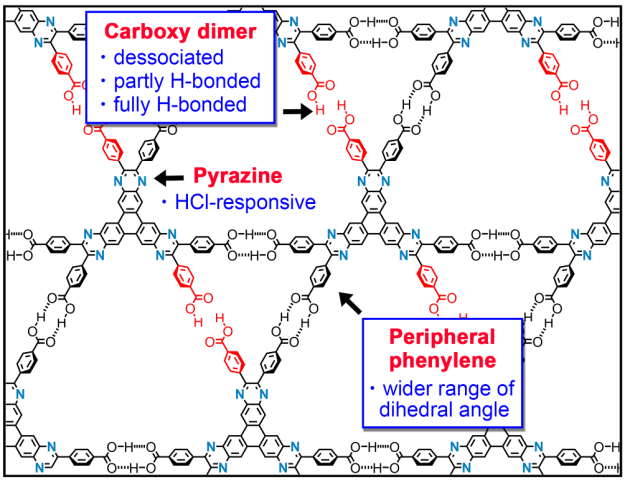

Figure 1. Schematic representation of hydrogen-bonded hexagonal network (H-HexNet) of **CPBTQ** and its features.

Results and Discussion

Synthesis and crystallization of CPBTQ. 2,3,6,7,10,11-Hexaaminotriphenylene hydrochloride salt, which was synthesized from the corresponding hexabromotriphenylene derivative according to the literature,[44] was treated by benzil derivative **1** in acetic acid to give ester derivative **2** (Scheme 1). **CPBTQ** was subsequently prepared by hydrolysis of **2**. **CPBTQ** was characterized by ^{1}H and ^{13}C NMR spectroscopy, HR-MS, and crystallographic analysis. Solvated framework **CPBTQ-1(MeBz)** with a H-HexNet motif was obtained as needle-shaped orange crystals by slow evaporation of a solution of **CPBTQ** dissolved in *N*,*N*-dimethylacetamide (DMA) and methyl benzoate (MeBz) at 120 °C for 3 days. We also attempted

to obtain a crystal of **CPBTQ** with the same solvent system (i.e. *N*-methylpyrrolidone and 1,2,4-trichlorobenzene) as in the case of **CPHATN**. However, no crystal was obtained.

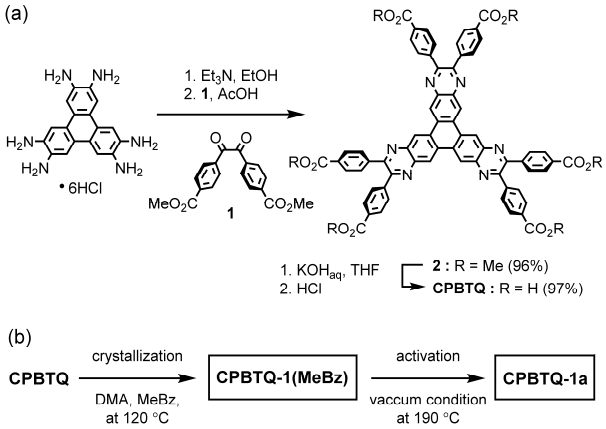

Scheme 1. (a) Synthesis and (b) crystallization of **CPBTQ**

Crystal structure of CPBTQ-1(MeBz). CPBTQ crystallized into the space group of $P3_212$ (no.153) to give the solvated H-HexNet framework, **CPBTQ-1(MeBz)**, as shown in Figure 2 and Table S1. The crystal consists of four symmetrically-independent molecules of **CPBTQ** (A, B, C, and D), two of which possess C_2-symmetric axis (A and D). Since C_2-symmetric axis lies on the center of carboxy dimer, the hydrogen atoms are expediently attached on both the oxygen atoms of the carboxy group as shown in Figure S1. BTQ cores are slightly deformed due to the packing force in solid state: root mean square deviation (RMSD) of the cores ranges from 0.06 to 0.19 Å (Table 1). **CPBTQ** molecules (A–D) are stacked along the *c* axis with three-fold helical manner, and each of them respectively forms a perfect or quasi H-HexNet sheet. In contrast with the previously reported HOF **CPHATN-1(124TCB)**, H-HexNets of **CPBTQ-1(MeBz)** involve a dissociated dimer (dd) and defective H-bonded dimers such as an open dimer (od) and truncated chain (tc), in addition to perfectly H-bonded dimer of the carboxy groups as shown in Figures 2b and 3. These defective H-bonded dimers has open-end hydroxy groups, which are probably

trapped by solvent molecules through H-bonds[36] although most of solvent molecules were not able to be solved crystallographically due to sever disorder. It is noteworthy that anisotropic displacement of the peripheral carboxyphenyl groups is much more significant than that of the BTQ core moiety: Averaged U_{iso} values for cores A, B, C, and D range from 0.053 to 0.062, while those of phenylene moieties and carboxy groups range from 0.080 to 0.11, and from 0.123 to 0.143, respectively (Table 1). Particularly, the groups with defectively H-bonded or dissociated dimers are severely disordered (Figure S2). H-HexNet frameworks stacked nearly in an eclipsed manner between layers B and C. In the cases of layers A-B and C-D, on the other hand, the H-HexNet layers stack in an inverted fashion, resulting less overlap of the frameworks. The defective H-bonded dimers and highly disordered atoms with larger U_{iso} exist in these less-overlapped regions. The imperfect H-bonded network formation in **CPBTQ-1(MeBz)** effects on stability of the framework as described later. The framework has two kinds of threefold helical channels (I and II) along the crystallographic *b* axis (Figure 4). In the channels, MeBz molecules are accommodated thought they are highly disordered, and therefore, most of them are not able to characterized crystallographically (Figure S3). Channel I has a narrow width of 5 Å and unlevel surface. Channel II has a more complicated shape, like a shish-kebab structure, with narrow bottle neck (7 Å) and wide discotic spaces (20 Å). A ratio of total potential solvent area volume is calculated to be 36% by PLATON software with probe radius of 1.2 Å (cell volume: 34267.5 $Å^3$, void volume per cell: 12418 $Å^3$).

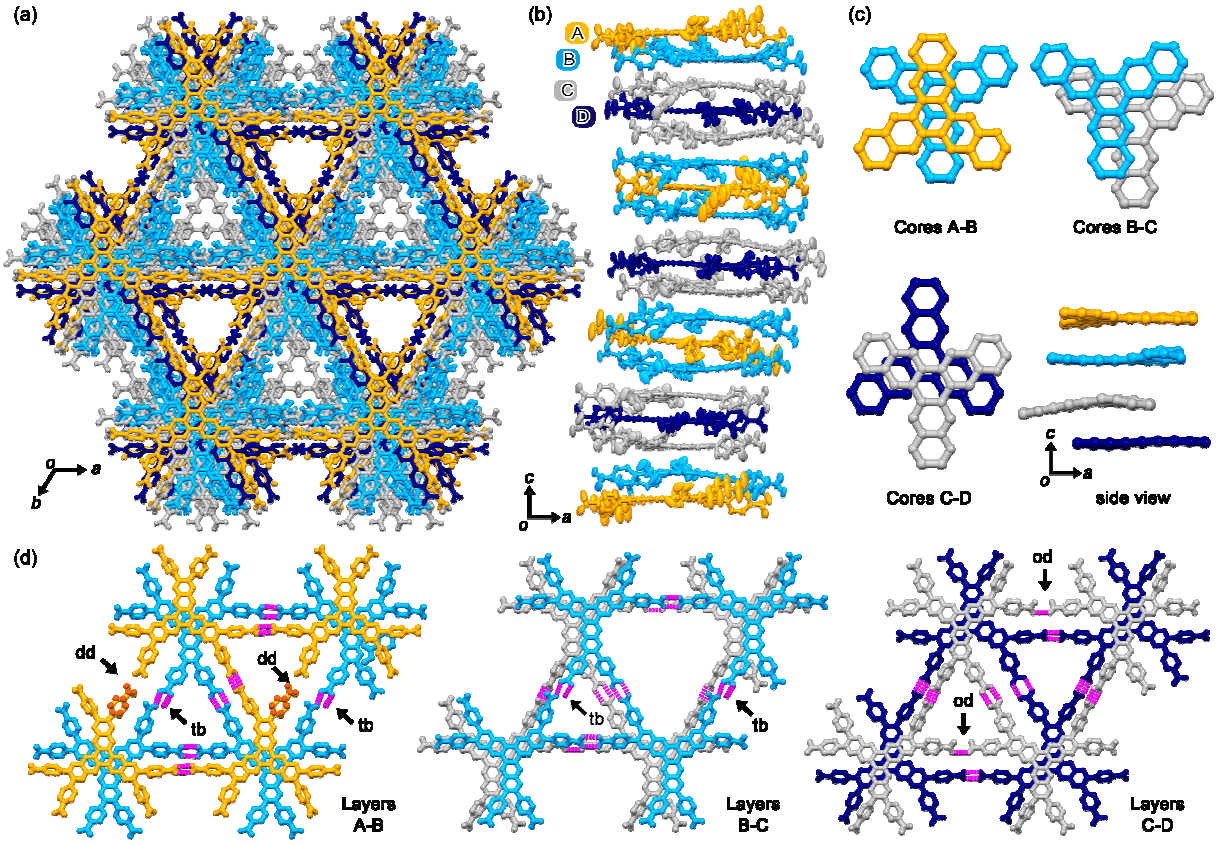

Figure 2. Crystal structure of **CPBTQ-1(MeBz)**. (a) Packing diagram viewed down from the *c* axis. (b) Side view of stacked molecules in the unit cell drawn by displacement anisotropic ellipsoids with 50% probability, where four symmetrically-independent molecules (A, B, C, and D) are colored by yellow, cyan, gray, and dark blue, respectively. A and D have C_2-axis within the molecules. (c) Relative positions of the stacked BTQ cores. (d) Stacking motifs of the adjacent layeres A-B, B-C, and C-D. Dash lines in magenta denote H-bonds. Orange spheres in layer A denote the other part of the carboxyphenyl groups disordered in two positions. dd: dissociated dimer, tc: truncated H-bonded chain, od: open dimer.

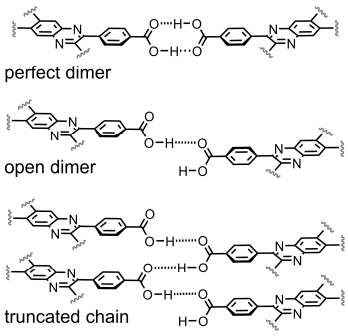

Figure 3. H-bonding patterns of carboxy groups observed in a crystal structure of **CPBTQ-1(MeBz)**.

Table 1. Structural displacement parameters of **CPBTQ** molecules A, B, C, and D.

	A[a]	B	C	D
RMSD of BTQ core[b]	0.10	0.18	0.19	0.06
U_{iso}(BTQ core)[c]	0.062	0.053	0.054	0.050
U_{iso}(phenylene)[c]	0.107	0.084	0.080	0.080
U_{iso}(carboxy)[c]	0.143	0.128	0.123	0.132

[a] Values for one of the symmetrically-independent three carboxyphenyl groups are not included due to its significantly disordered structure, which is refined with structural restrain.

[b] Root mean square deviation (RMSD) of BTQ moiety.

[c] Averaged values of U_{iso} are applied.

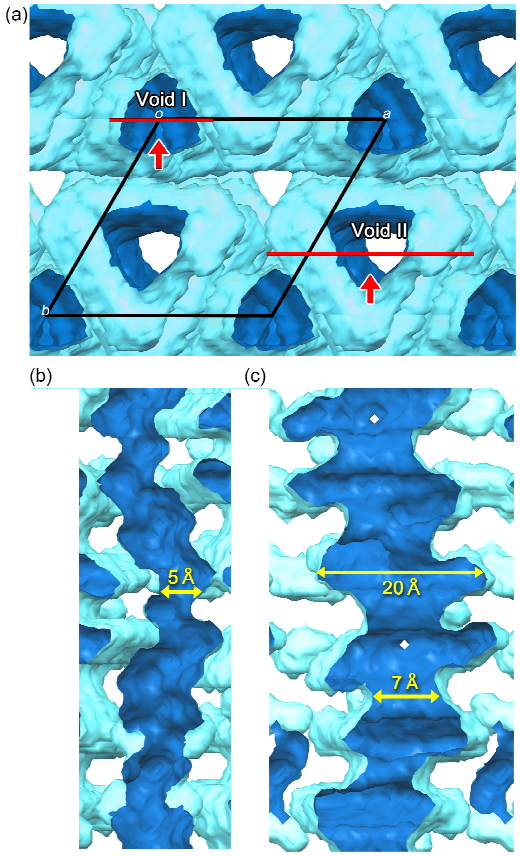

Figure 4. Visualized surfaces of the void. (a) Top view of the voids. (b) Cross-section of the channel I. (c) Cross section of the channel II. The cross-section images were prepared by cutting on the red lines and viewing from a direction along red arrows.

Comparison between CPHATN and CPBTQ crystals. As previously reported, **CPHATN**, which is an isomer of **CPBTQ**, is crystallized into *P*-1 space group with *Z*` = 1 (Figure S4). The structural differences between molecules **CPHATN** and **CPBTQ** is location of the pyrazine rings as shown in Chart 1. This difference, however, caused crucial differences on their molecular packing in crystalline states. These differences can be explained from conformation of the peripheral phenylene moieties. Figure 5 shows distribution of dihedral angle (ϕ) of biphenyl derivatives with *ortho*-substituents and of 2-phenyl-3-substituted-pyridine derivatives, where

substituent R is phenyl group or *o*-, *m*-, and/or *p*- substituted phenyl groups, surveyed by Mogul, which is a knowledge-based library of molecular geometry derived from the Cambridge Structural Database.[45,46] Distribution of the dihedral angle in the phenyl-pyridine systems slightly shifted into smaller angle region for ϕ <90° and into larger angle region for ϕ >90° compared with the phenyl-benzene systems due to less steric hindrance at the *ortho*-position (i.e. C–H vs. N). These results indicate that phenyl-pyridine systems have larger degree of freedom regarding rotational conformations. Indeed, the ϕ values observed in HOFs and Nπ-HOFs composed of C_3PIs **Tp**, **CPHAT**, **CPHATN**, and **CPBTQ** show the same tendency (Table 2). HOFs **Tp-1**, **-2**, **-3**, **-4**, and **CPHATN-1a** exhibit the angle ϕ ranging from 43.7 to 72.8°. On the other hand, that of HOFs **CPHAT-1a** and the present **CPBTQ-1(MeBz)** ranges from 27.9 to 65.6°. High degree of freedom on conformation of the peripheral phenylene groups, in the case of **CPBTQ**, results in increase of versatility of molecular packing pattern, to yield the framework with high *Z*' values and partly defected H-bonding network. Additionally, in the crystal structure of **CPBTQ-1(MeBz)**, interlayer CH···N interactions form between the N atoms in the BTQ core and aromatic proton of the phenylene groups of **CPBTQ** located in the next stacked layer: [C(197)–H···N(11): H···N distance: 2.62 Å, C–H–N angle: 157.7°. C(164)–H···N(16): H···N distance: 2.58 Å, C–H–N angle: 164.5°] (Figure S5). Because of these interlayer C–H···N contacts, the involved phenylene rings have more twisted conformation with larger values of ϕ (ϕ = 65.6° and 49.4°). In the case of **CPHATN**, on the other hand, the N atoms in the core are difficult to make interlayer C–H···N interactions due to steric hindrances.

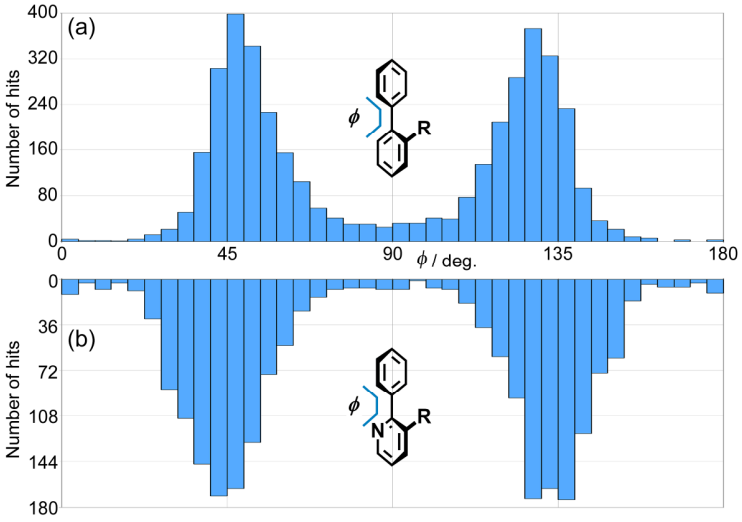

Figure 5. Dihedral angle distribution of (a) phenyl-benzene and (b) phenyl-pyridine systems possessing substituents at the *ortho*-position of the phenyl group.

Table 2. Dihedral angles ϕ in Nπ-HOFs **CPBTQ-1(MeBz)** and the related crystals.

crystal	ϕ [a] [°]
Tp-1, **-2**, **-3**, and **-4**	49.8–72.8 (56.2)[b]
CPHATN-1a	43.7–67.6 (52.8)[b]
CPHAT-1a (124TCB)	27.9
CPBTQ-1(MeBz) (A)	34.9–65.6 (49.9)[b]
(B)	38.3–49.4 (45.5)[b]
(C)	33.3–56.4 (42.6)[b]
(D)	38.2–57.6 (48.9)[b]

a Ranges of ϕ

b Values in the parentheses are averaged angle of ϕ.

Thermal behaviors. Thermal gravimetric (TG) analysis of as-formed crystalline bulk of **CPBTQ-1(MeBz)** shows two weight loss process (Figure S6), indicating that the MeBz molecules are located at least two different positions through different intermolecular interactions. Indeed, crystallographic analysis were capable of solving symmetrically independent one MeBz molecule, which was stacked at the corner of the void, while the other MeBz molecules were not due to sever disorder as shown in Figure S3. Consequently, solvent molecules inside the framework were completely removed at around 240 °C under ambient pressure. To reveal structural changes of **CPBTQ-1(MeBz)** during desolvation by heating, powder X-ray diffraction (PXRD) patterns of crystalline bulk were recorded as gradually heated upto 360 °C (Figure 6). Although initial intensity of the diffraction peaks are weak due to sever disorder of solvent molecules inside voids,[38] peaks at 3.92° as well as ca. 6.8° and 7.8° gradually appeared, and grew up to 210 °C by heating. The resultant pattern is in good agreement with the original pattern of **CPBTQ-1(MeBz)**, indicating that the desolvated material retains its original framework. At higher temperature than 210 °C, however, the peaks became broader and weaker, indicating that crystallinity of the bulk was gradually lost. These results are consistent with the complicated crystal structure of **CPBTQ-1(MeBz)** containing as many as four symmetrically-independent molecules and a defective H-boned network. With these results in mind, activation of the material was accomplished by heating at 190 °C for 48 h under a vacum condition, giving the corresponding desolvated materials **CPBTQ-1a**. Complete desolvation and crystallinity of the activated materials were confirmed by ^{1}H NMR spectra of solutions dissolved in dueterated DMSO (Figure S7) and PXRD patterns (Figure S8), respectively.

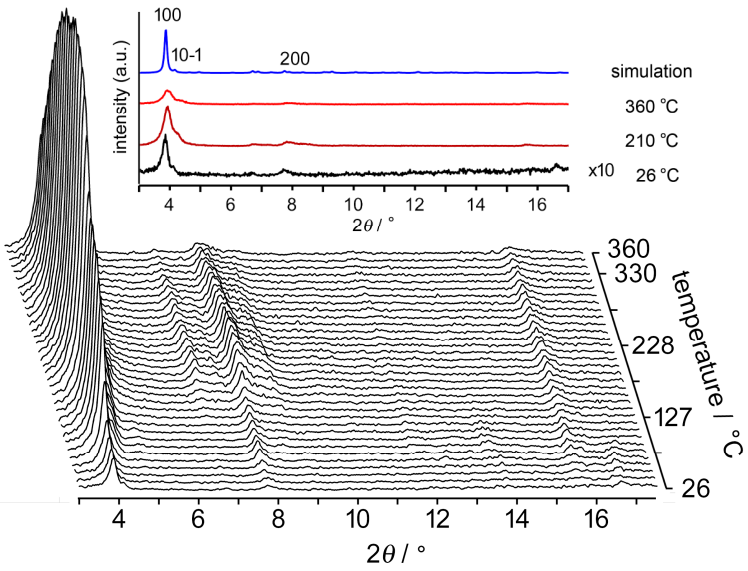

Figure 6. Variable temperature (VT) PXRD patterns of crystalline bulk of as-formed **CPBTQ-1**. Temperature was increased at the rate of 1 °C min^{-1}. PXRD patterns were recorded from 3° to 18° of 2θ with the scan rate of 3°min^{-1}. Therefore, each scan has a temperature gradient of 5 °C. The inserted PXRD pattern at 26 °C is magnified 10 times for clarity.

Evaluation of permanent porosity. CPBTQ-1a shows type-I or quasi-type-I isotherms for N_2, CO_2, H_2, and O_2 sorption at low temperature. The uptakes are 125 cm^3/g for N_2 at 101.5 kPa, 147.7 cm^3g^{-1} for O_2 at 20.9 kPa, 135 cm^3g^{-1} for CO_2 at 100.4 kPa, and 57.5 cm^3g^{-1} for H_2 at 101.7 kPa. Calculated BET surface area and pore volume based on the CO_2 sorption isotherm are 471 m^2g^{-1} and 0.3721 cm^3g^{-1}, respectively (Figure S9). Pore size distribution of **CPBTQ-1a** calculated by the non-localized density functional theory (NLDFT) shows two peaks at 0.7 nm and 1.1 nm (Figure S10), supporting the complex shape of the void channels in **CPBTQ-1a** as shown in Figure 4. It is noteworthy that N_2 sorption processes of **CPBTQ-1a** undertook much more slowly compared with the case of **CPHATN-1a**.[44] This result is also supported by the crystal structure of **CPBTQ-1(MeBz)** possessing narrower bottle neck of the 1D channels.

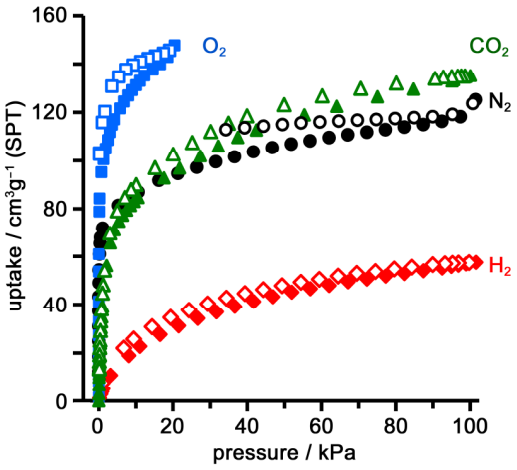

Figure 7. Gas sorption isotherms of **CPBTQ-1a** at low temperature. Nitrogen (black circle) at 77K, carbon dioxide (green triangle) at 195 K, oxygen (blue squre) at 77K, and hydrogen (red diamond) at 77K. Solid symbol: absorption. Open symbol: desorption.

Struture durability toward common solvents. To disclose structural durability of the frameworks toward common solvents, crystalline powder of **CPBTQ-1a** was immersed into hot solvents [chloroform (60 °C), toluene (100 °C), ethanol (60 °C), and water (100°C)] for 24 h, filtered, and subjected to PXRD measurement (Figure 8). The original pattern was also retained and the peak intensity was recovered after heating, except for the case of water and conc.HCl, in which recovery of the peak intensity was prevented. These results indicate that **CPBTQ-1a** is stable toward less polar organic solvent but is not stable suficiently toward highly polar solvents, which is in contrast to **CPHATN-1a**.

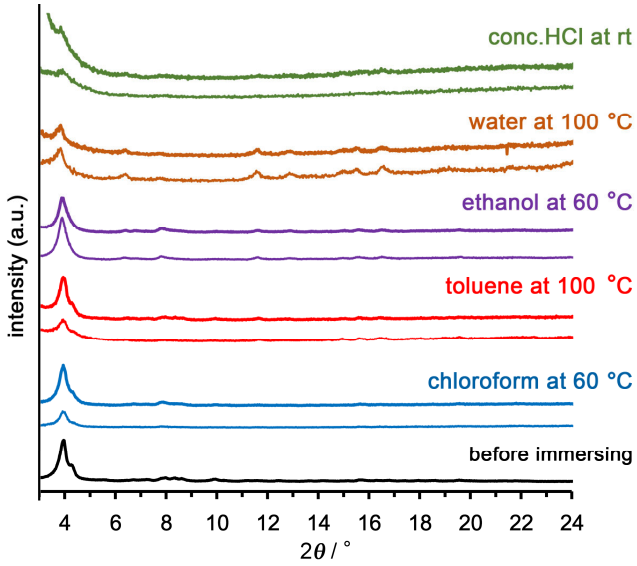

Figure 8. PXRD patterns of crystalline bulk of **CPBTQ-1a** before and after immersed into hot solvents and ambient conc. HCl for 24 h. Bottom lines: wet materials obtained just after filteration. Top lines: dried materials obtained after heating the filtered samples at 150 °C for 1h to remove the solvents.

Acid-induced Color changes. Since **CPBTQ** has three pyrazine rings annelated to triphenylene core, the corresponding HOF **CPBTQ-1a** exhibits HCl responsivness as in the cases of **CPHATN-1a**[43] and **CBPHAT-1a**.[47] As shown in Figure 9a, yellow-brown crystalline bulks of **CPBTQ-1a** immideately turned into redish-brown by adding a drop of conc. HCl aqueous solution. In solid state absorption spectrum of **CPBTQ-1a** (Figure 9b), absorpion shoulder at aroud 550–600 nm is observed after adding HCl. Subsequence heating of the brown bulks resulted in recovery of the original color due to removal of HCl. To obtain structural

information of **CPBTQ-1a** upon exposure to HCl, PXRD patterns of the crystalline bulk were recorded before and after added a drop of conc. HCl, and after removeal of HCl by heating for 30 min at 150 °C as shown in Figure 9c. The PXRD patterns were once disappered by adding a HCl drop. The original pattern was then slightly recovered by heating, implying that addition of HCl to the framework may perturbe the crystal structure through rearrangement or exchanges of H-bonding. This observation is also contrary to **CPHATN-1a** with a rigid framework.

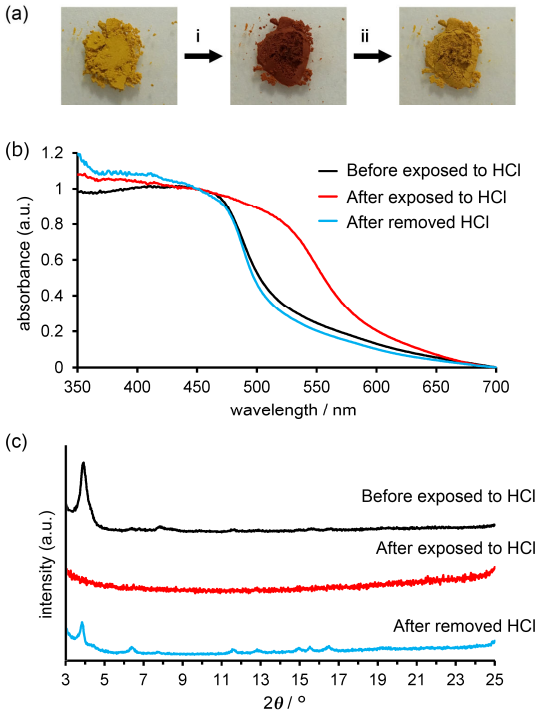

Figure 9. HCl responsiveness of **CPBTQ-1a**. (a) Color changes of crystalline bulk upon exposing to HCl. Conditions: (i) adding a drop of conc. HCl on the materials, (ii) heating at 150 °C for 30 min. Changes on (b) absorption spectra and (c) PXRD patterns upon exposing to HCl and subsequent removing of HCl.

Conclusion

In this study, A porous hydrogen-bonded organic framework (HOF) composed of N-hetero π-conjugated molecules (Nπ-HOF) was constructed from carboxyphenyl-substituted benzotriquinoxaline derivative (**CPBTQ**). The resultant solvated framework **CPBTQ-1(MeBz)** consists of layered 2D hexagonal network sheet, which was precisely revealed by single-crystalline X-ray diffraction analysis. Compared with the previously reported Nπ-HOF composed of isomer hexaazatrinaphthylene derivative (**CPHATN**) possessing pyrazine rings in the different positons, the present framework has a complicated and defective H-bonded network structure. We thoroughly studied the positional effects of the pyrazine rings on the structure, and revealed that that the positional difference strongly effects on conformation of the peripheral phenylene groups. The dihedral angles of the peripheral phenylene rings (ϕ) can range wider in the case of **CPBTQ** (33.3−65.6°) than **CPHATN** (43.7–67.6°) due to less steric hindrance at the *ortho*-positions. Permanent porosity, thermal and chemical stabilities, and reversible HCl responsiveness of the activated Nπ-HOF **CPBTQ-1a** were also evaluated. We believe that the present results can contribute not only for construction of new functional Nπ-HOFs, but also for chemistry on hetero-aromatic compounds.

Experimental Section.

General. All reagents and solvents were used as received from commercial suppliers. ^{1}H and ^{13}C NMR spectra were measured by JEOL 400 YH (400 MHz) spectrometer. Residual proton and carbon of deuterated solvents were used as internal standards for the measurements (for ^{1}H NMR, $CDCl_3$, δ = 7.26 ppm; DMDO-d_6, δ = 2.49 ppm: for ^{13}C NMR, $CDCl_3$, δ = 77.00 ppm; DMSO-d_6, δ = 39.50 ppm). Mass spectrum data were obtained from a autoflex III Bruker. Thermo gravimetric (TG) analysis were performed on Rigaku TG8120 under an N_2 purge (100 mL

min^{-1}) at a heating rate of 5 $Kmin^{-1}$. Powder X-ray diffraction (PXRD) data were collected on a Rigaku Ultima-IV (40 kV, 44 mA) using graphite-monochromatized Cu-*Kα* radiation (λ = 1.54187 Å) at room temperature. A scan rate is 2.0 ° min^{-1}. **Single crystal X-ray measurement and analysis.** Diffraction data of **CPBTQ-1** was collected on a CCD (MX225HE, Rayonix) with the synchrotron radiation (λ = 0.8500 Å) monochromated by the fixed exit Si (111) double crystal. The cell refinements were performed with a software CrysAlisPro.[48] SHELXT[49] was used for the structure solution of the crystals. All calculations were performed with the observed reflections [I > 2σ(I)] with the program CrystalStructure crystallographic software packages, except for refinement which was performed by SHELXL.[50] All non-hydrogen atoms were refined with anisotropic displacement parameters, and hydrogen atoms were placed in idealized positions and refined as rigid atoms with the relative isotropic displacement parameters. SQUEEZE function equipped in the PLATON softeware[51,52] was used to remove severely disordered solvent molecules in voids (CCDC number of **CPBTQ-1**: 1976117). **Variable temperature (VT) PXRD measurement.** Crystalline bulk of **CPBTQ-1** placed on an aluminum substrate was subjected to VT-PXRD measurement under the air atmosphere. PXRD data were collected on a Rigaku Ultima-IV using graphite-monochromatized Cu-Kα radiation (λ = 1.54187 Å) with a temperature control unit. Temperature of the sample was increased from room temperature to 633 K with a rate of 1 K/min. During temperature increasing, XRD patterns ranged from 2° to 17° was repeatedly recorded with a scan rate of 3 ° min^{-1}. Therefore, each PXRD scan has a temperature width of 5 K. **Sorption/desorption experiment.** Activation of **CPBTQ-1(MeBz)** was performed under vacuum condition (0.2 kPa) for 48h at 463 K to give **CPBTQ-1a** for sorption experiments. Gas sorption measurements were performed on

BELSORP-max (BEL, Japan). The adsorption isotherms of N_2, O_2, CO_2, and H_2 were corrected at 77K, 77 K, 195 K and 77 K, respectively.

Methyl ester 2. To a mixture of 2,3,6,7,10,11-hexaaminotriphenylene HCl salt[44] (747 mg, 1.39 mmol) in dry EtOH (100 mL) was added dropwise triethylamine (1.0 g). The reaction mixture was stirred for 10 min. To the reaction mixture was added benzyl derivative **1** (1.54 g, 4.72 mmol) and acetic acid (2 mL), and the mixture was stirred for 24 h under reflux condition. The dark green suspension turned into a brown one. After cooled to room temperature, the precipitate was collected by centrifuge, washed with EtOH and THF, and dried in vacuo to give **2** (1.59 g, 96%) as an orange solid. Mp. >300 °C. ^{1}H NMR (400 MHz, $CDCl_3$) δ 9.12 (s, 6H), 8.03 (d, J = 8.0 Hz, 12H), 7.65 (d, J = 8.4 Hz, 12H), 3.99 (s, 18H) ppm. ^{13}C NMR (100 MHz, $CDCl_3$) δ 166.5, 153.5, 142.6, 140.4, 131.8, 130.8, 130.0, 129.6, 124.9, 52.4 ppm. HR-MS (MALDI) *m/z* calc. for $[M]^-$ $C_{72}H_{48}N_6O_{12}$: 1188.3372; found: 1188.3330.

CPBTQ. Ester **2** (1.08 g, 0.908 mmol) and KOH (1.00 g, 17.8 mmol) in 1,4-dioxane (70 mL) and water (130 mL) was stirred for 48 h under reflux condition. The reaction mixture was passed through a filter paper and the filtrate was acidized with 2M HCl. The resulting precipitate was corrected by centrifuge, washed with water, EtOH, and THF, and dried in vacuo to give CPBTQ (974 mg, 97%) as a dark orange solid. Mp. >300 °C. ^{1}H NMR (400 MHz, DMSO-d_6, 70 °C) δ 8.08 (s, 6H), 7.81 (d, J = 8 Hz, 12H), 7.30 (d, J = 7.6 Hz, 12H) ppm. ^{13}C NMR (100 MHz, DMSO-d_6, 25 °C) δ 166.75, 152.24, 141.75, 139.51, 134.04, 130.84, 129.77, 128.75, 124.87 ppm. HR-MS (MALDI) *m/z* calc. for $[M]^-$ $C_{66}H_{36}N_6O_{12}$: 1104.2391; found: 1104.2407.

Acknowledgement

This work is supported by a Grant-in-Aid for Scientific Research (B) (JP18H01966) and for Scientific Research on Innovative Area “Coordination Asymmetry” (No. JP19H04557) from MEXT Japan. X-ray diffraction data, including preliminary data sets, were collected at BL38B1, BL40XU, and BL26B1 in SPring-8 with approval of JASRI (proposal Nos. 2017B1322, 2018A1327, 2018B1244, 2019A1192, 2019B1738). The authors thank to Mr. Y. Suzuki at Osaka University for NMR measurements.

.

ASSOCIATED CONTENT

Supporting Information.

The following files are available free of charge.

Details of crystal structures of **CPBTQ-1(MeBz)** and thermal, diffraction, and spectroscopic analyses (PDF)

X-ray data for **CPBTQ-1(MeBz)** (CIF)

AUTHOR INFORMATION

Corresponding Author

*hisaki@chem.es.osaka-u.ac.jp

Funding Sources

Grant-in-Aid for Scientific Research (B) (JP18H01966) and for Scientific Research on Innovative Area “Coordination Asymmetry” (No. JP19H04557) from MEXT Japan.

ACKNOWLEDGMENT

This work is supported by a Grant-in-Aid for Scientific Research (B) (JP18H01966) and for Scientific Research on Innovative Area “Coordination Asymmetry” (No. JP19H04557) from MEXT Japan. X-ray diffraction data, including preliminary data sets, were collected at BL38B1, BL40XU, and BL26B1 in SPring-8 with approval of JASRI (proposal Nos. 2017B1322, 2018A1327, 2018B1244, 2019A1192, 2019B1738). The authors thank to Mr. Y. Suzuki at Osaka University for NMR measurements.

REFERENCES

1. Richards, G. J.; Hill, J. P.; Subbaiyan, N. K.; D’Souza, F.; Karr, P. A.; Elsegood, M. R. J.; Teat, S. J.; Mori, T. Ariga, K. Pyrazinacenes: Aza Analogues of Acenes. *J. Org. Chem.* **2009**, 74, 8914–8923.

2. Bunz, U. H. F. N-Heteroacenes. *Chem. Eur. J.* **2009**, *15*, 6780–6789.

3. Richards, G. J. Cador, A.; Yamada, S.; Middleton, A.; Webre, W. A.; Labuta, J.; Karr, P. A.; Ariga, K.; D’Souza, F.; Kahlal, S.; Halet, J.-F.; Hill, J. P. Amphiprotism-coupled near-infrared emission in extended pyrazinacenes containing seven linearly fused pyrazine units. *J. Am. Chem. Soc.* **2019**, *141*, 19570−19574.

4. Bunz, U. H. F.; Freudenberg, J. *Acc. Chem. Res*. **2019**, *52*, 1575–1587.

5. Segura, J. L.; Juárez, R.; Ramos, M.; Seoane, C. Hexaazatriphenylene (HAT) derivatives: from synthesis to molecular design, self-organization and device applications. *Chem. Soc. Rev.* **2015**, *44*, 6850−6885.

6. Takase, M.; Enkelmann, V.; Sebastiani, D.; Baumgarten, M.; Müllen, K. Annularly fused hexapyrrolohexaazacoronenes: An extendedp system with multiple interior nitrogen atoms displays stable oxidation states. *Angew. Chem. Int. Ed.* **2007**, *46*, 5524−5527.

7. Oki, K.; Takase, M.; Mori, S.; Uno. H. Synthesis and isolation of antiaromatic expanded azacoronene via intramolecular vilsmeier-type reaction. *J. Am. Chem. Soc*. **2019**, *141*, 16255−16259.

8. Saito, M.; Shinokubo, H.; Sakurai, H.; Figuration of bowl-shaped π-conjugated molecules: properties and functions. : *Mater. Chem. Front.* **2018**, *2*, 635−661.

9. Yokoi, H.; Hiraoka, Y.; Hiroto, S.; Sakamaki, D.; Seki, S.; Shinokubo, H. Nitrogen-embedded buckybowl and its assembly with C_{60}. *Nat. Commun.* **2015**, *6*, 8215.

10. Tan, O.; Higashibayashi, S.; Karanjit, S.; Hidehiro Sakurai, H. Enantioselective synthesis of a chiral nitrogen-doped buckybowl. *Nat. Commun.* **2012**, *3*, 891.

11. Scipioni, R.; Boero, M.; Richards, G. J.; Hill, J. P.; Ohno, T.; Mori, T.; Ariga, K. Tautomerism in reduced Pyrazinacenes. *J. Chem. Theory Comput.* **2010**, *6*, 517−525.

12. He, Z.; Mao, R.; Liu, D.; Miao, Q. Highly electron-deficient hexaazapentacenes and their dihydro precursors, *Org. Lett*. *14*, **2012**, *14*, 4190−4193.

13. Fleischhauer, J.; Zahn, S.; Beckert, R.; Grummt, U.-W.; Birckner, E.; Gçrls, H. A way to stable, highly emissive fluorubine dyes: Tuning the electronic properties of azaderivatives of pentacene by introducing substituted pyrazines, *Chem. Eur. J.* **2012**, 18, 4549–4557.

14. Lakshminarayana, A. N.; Ogn, A.; Chi, C.; Modification of acenes for n-channel OFET materials. *J. Mater. Chem. C.* **2018**, *6*, 3551−3563.

15. Nie, B.; Zhan, T.-G.; Zhou, T.-Y.; Xian, Z.-Y.; Jiang, G.-F.; Zhao, X., Self-assembly of chiral propeller-like supermolecules with unusual "sergeants-and-soldiers" and "majority-rules" effects. *Chem. Asian J.* **2014**, *9*, 754–758.

16. Li, J.; Chen, S.; Zhang, P.; Wang, Z.; Long, G.; Ganguly, R.; Li, Y.; Zhang, Q., A colorimetric and fluorimetric chemodosimeter for copper ion based on the conversion of dihydropyrazine to pyrazine. *Chem. Asian J*. **2016**, *11*, 136–140.

17. Catalano, V. J.; Larson, W. E.; Olmstead, M. M.; Gray, H. B., Mononuclear and binuclear palladium(II)/rhenium(I) complexes containing a sterically hindered trinucleating Ligand: 2,3,8,9,14,15-Hexamethyl-5,6,11,12,17,18-hexaazatrinaphthalene (hhtn) *Inorg. Chem*. **1994**, *33*, 4502–4509.

18. Piglosiewicz, I. M.; Beckhaus, R.; Saak, W.; Haase D., Dehydroaromatization of quinoxalines: one-step syntheses of trinuclear 1,6,7,12,13,18-hexaazatrinaphthylene titanium complexes. *J. Am. Chem. Soc*. **2005**, *127*, 14190–14191.

19. Roy, S.; Sarkar, B.; Duboc, C.; Fiedler, J.; Sarper, O.; Lissner, F.; Mobin, S. M.; Lahiri, G. K.; Kaim, W., Heterohexanuclear (Cu_3Fe_3) complexes of substituted hexaazatrinaphthylene (HATN) ligands: twofold BF_4^- association in the solid and stepwise oxidation (3e) or reduction (2e) to spectroelectrochemically characterized species. *Chem. Eur. J*. **2009**, *15*, 6932–6939.

20. Fraser, M. G.; Clark, C. A.; Horvath, R.; Lind, S. J.; Blackman, A. G.; Sun, X.-Z.; George, M. W.; Gordon, K. C., Complete family of mono-, bi-, and trinuclear $Re(I)(CO)_3Cl$ complexes of the bridging polypyridyl ligand 2,3,8,9,14,15-hexamethyl-5,6,11,12,17,18-

hexaazatrinapthalene: syn/anti isomer separation, characterization, and photophysics. *Inorg. Chem*. **2011**, *50*, 6093–6106.

21. Bu, X.-H.; Biradha, K.; Yamaguchi, T.; Nishimura, M.; Ito, T.; Tanaka, K.; Shionoya, M., A novel polymeric AgI complex consisting of two three-dimensional networks which are enantiometric and interpenetrating. *Chem. Commun*. **2000**, 1953–1954.

22. Winkler, M.; Houk, K. N., Nitrogen-rich oligoacenes: Candidates for n-channel organic semiconductors. *J. Am. Chem. Soc.* **2007**, 129, 1805–1815.

23. Tadokoro, M.; Yasuzuka, S.; Nakamura, M.; Shinoda, T.; Tatenuma, T.; Mitsumi, M.; Ozawa, Y.; Toriumi, K.; Yoshino, H.; Shiomi, D.; Sato, K.; Takui, T.; Mori, T.; Murata, K. A high-conductive crystal containing a copper (I) coordination polymer bridged by the organic acceptor TANC, *Angew. Chem. Int. Ed.*, **2006**, *45*, 5144–5147.

24. Thusek, J.; Hoffmann, M.; Hebner, O.; Tverskoy, O.; Bunz, U. H. F.; Dreuw, A.; Himmel, H.-J., Low-energy electronic excitations of N-substituted heteroacene molecules: matrix isolation spectroscopy in concert with quantum-chemical calculations, *Chem. Eur. J.* **2019**, *25*, 15147–15154.

25. Campbell, J. E.; Yang, J.; Day, G. M., Predicted energy–structure–function maps for the evaluation of small molecule organic semiconductors. *J. Mater. Chem. C* **2017**, 5, 7574–7584.

26. Chen, H.-Y.; Chao, I., Toward the rational design of functionalized pentacenes: reduction of the impact of functionalization on the reorganization energy. *ChemPhysChem* **2006**, *7*, 2003–2007.

27. Isoda, K.; Matsuzaka, M.; Sugaya, T.; Yasuda, T.; Tadokoro, M., Synthesis and electrochromic behavior of a multi-electron redox-active N-heteroheptacenequinone. *Org. Biomol. Chem.* **2019**, *17*, 7884–7890.

28. Georgiou, I.; Kervyn, S.; Rossignon, A.; De Leo, F.; Wouters, J.; Bruylants, G.; Bonifazi, D. Versatile self-adapting boronic acids for H-bond recognition: from discrete to polymeric supramolecules. *J. Am. Chem. Soc.* **2017**, *139*, 2710–2727.

29. Lu, J., Cao, R., Porous organic molecular frameworks with extrinsic porosity: a platform for carbon storage and separation. *Angew. Chem. Int. Ed.* **2016**, *55*, 9474–9480.

30. Cooper A. I. Porous molecular solids and liquids. *ACS Cent. Sci*. **2017**, *3*, 544–553.

31. Han, Y.-F.; Yuan, Y.-X.; Wang, H.-B., Porous hydrogen-bonded organic frameworks. *Molecules* **2017**, *22*, 266.

32. Luo, J.; Wang, J.-W.; Zhang, J.-H.; Lai, S.; Zhong, D.-C., Hydrogen-bonded organic frameworks: design, structures and potential applications. *CrystEngComm* **2018**, *20*, 5884–5898.

33. Lin, R.-B.; He, Y.; Ki, P.; Wang, H.; Zhou, W.; Chen, B., Multifunctional porous hydrogen-bonded organic framework materials. *Chem. Soc Rev.* **2019**, *48*, 1362–1389.

34. Hisaki, I.; Chen, X.; Takahashi, K.; Nakamura, T., Designing hydrogen-bonded organic frameworks (HOFs) with permanent porosity. *Angew. Chem. Int. Ed*. **2019**, *58*, 11160–11170.

35. Positional effects of the carboxy groups on frameworks are studied, see; a) Takeda, T.; Ozawa, M.; Akutagawa, T., Jumping crystal of a hydrogen-bonded organic framework induced by the collective molecular motion of a twisted π system. *Angew. Chem. Int. Ed.*

2019, *58*, 10345–10352. b) Takeda, T.; Ozawa, M.; Akuagawa, T., Versatile hydrogen-bonded assemblies of twisted tetra[3,4]thienylene tetracarboxylic acid with Selective solvent sorption. *Cryst. Growth Des.* **2019**, *19*, 4784–4792.

36. Hisaki, I.; Nakagawa, S.; Tohnai, N.; Miyata, M., A C_3-symmetric macrocycle-based, hydrogen-bonded, multiporous hexagonal network as a motif of porous molecular crystals. *Angew. Chem. Int. Ed.* **2015**, *54*, 3008–3012.

37. Hisaki, I.; Ikenaka, N.; Tohnai, N.; Miyata, M., Polymorphs of layered assemblies of hydrogen-bonded hexagonal networks caused by conforma-tional frustration. *Chem. Commun*. **2016**, *52*, 300–303.

38. Hisaki, I.; Nakagawa, S.; Ikenaka, N.; Imamura, Y.; Katouda, M.; Tashiro, M.; Tsuchida, H.; Ogoshi, T.; Sato, H.; Tohnai, N.; Miyata, M., A series of layered assemblies of hydrogen-bonded, hexagonal networks of C_3-symmetric π-conjugated molecules: a potential motif of porous organic materials. *J. Am. Chem. Soc*. **2016**, *138*, 6617–6628.

39. Yang, W.; Zhou, W.; Chen, B. A flexible microporous hydrogen-bonded organic framework. *Cryst. Growth Des.* **2019**, *19*, 5184–5188.

40. Zhang, X.; Li, L.; Wang, J.-X.; Wen, H.-M.; Krishna, R.; Wu, H.; Zhou, W.; Chen, Z.-N.; Li, B.; Qian, G.; Chen, B. Selective ethane/ethylene separation in a robust microporous hydrogen-bonded organic framework. *J. Am. Chem. Soc.* **2020**, *142*, 633–640.

41. Hisaki, I.; Ikenaka, N.; Gomez, E.; Cohen, B.; Tohnai, N.; Douhal, A. Hexaazatriphenylene-based hydrogen-bonded organic framework with permanent porosity and single-crystallinity. *Chem. Eur. J.* **2017**, *23*, 11611–11619.

42. Hisaki, I.; Suzuki, Y.; Gomez, E.; Cohen, B.; Tohnai, N.; Douhal, A., Docking strategy to construct thermostable, single-crystalline, hydrogen-bonded organic framework with high surface area. *Angew. Chem. Int. Ed*. **2018**, *57*, 12650–12655.

43. Hisaki, I.; Suzuki, Y.; Gomez, E.; Ji, Q.; Tohnai, N.; Nakamura, T.; Douhal, A. Acid Responsive Hydrogen-bonded Organic Framework. *J. Am. Chem. Soc*. **2019**, *141*, 2111–2121.

44. Lebkücher, A.; Wagner, C.; Hübner, O.; Kaifer, E. Himmel, H.-J. Trinuclear complexes and coordination polymers of redox-active guanidino-functionalized aromatic (GFA) Compounds with a triphenylene core. *Inorg. Chem.* **2014**, *53*, 9876–9896.

45. Bruno, I. J.; Cole, J. C.; Kessler, M.; Luo, J.; Motherwell, W. D. S. Purkis, L. H.; Smith, B. R.; Taylor, R.; Cooper, R. I.; Harris S. E.; Orpen, A. G., Retrieval of crystallographically-derived molecular geometry information. *J. Chem. Inf. Comput. Sci*., **2004**, *44*, 2133–2144.

46. Cottrell, S. J.; Olsson, T. S. G.; Taylor, R.; Cole J. C.; Liebeschuetz, J. W., Validating and understanding ring conformations using small molecule crystallographic data. *J. Chem. Inf. Model*. **2012**, *52*, 956–962.

47. Gomez, E.; Suzuki, Y.; Hisaki, I.; Moreno, M.; Douhal, A. Spectroscopy and dynamics of a HOF and its molecular units: remarkable vapors acid sensing. *J. Chem. Mater. C* **2019**, 7, 10818–10832.

48. Rigaku Oxford Diffraction (2015), Software CrysAlisPro 1.171.38.41o. Rigaku Corporation, Tokyo, Japan.

49. Sheldrick, G. M. SHELXT - Integrated space-group and crystal-structure determination. *Acta Crystallogr. A* **2015**, *71*, 3–8.

50. Sheldrick, G. M. Crystal structure refinement with SHELXL. *Acta Crystallogr. Sect. C* **2015**, *71*, 3–8.

51. van der Sluis, P.; Spek, A. L. BYPASS: an effective method for the refinement of crystal structures containing disordered solvent regions. *Acta Crystallogr. Sect. A* **1990**, *46*, 194–201.

52. Spek, A. L. Structure validation in chemical crystallography. *Acta Crystallogr. Sect. D* **2009**, *65*, 148–155.

For Table of Contents Use Only

Positional Effects of Annelated Pyrazine Rings on Structure and Stability of Hydrogen-bonded Frameworks of Hexaazatrinaphthylene Derivatives

Ichiro Hisaki, Qin Ji, Kiyonori Takahashi, Norimitsu Tohnai, Takayoshi Nakamura*

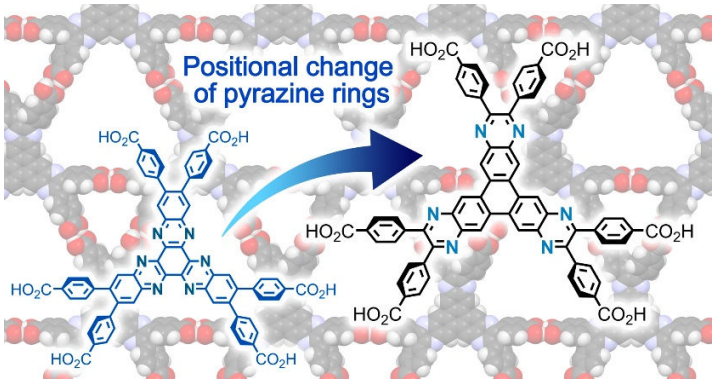

A new N-hetero π-conjugated molecule-based hydrogen-bonded organic framework (Nπ-HOF) was constructed. Comparison of Nπ-HOFs composed of two different isomer of hexaazanaphthylene revealed that the positional difference of the pyrazine rings strongly effects on conformation of the peripheral phenylene groups, which then lead to different structure and stability of the Nπ-HOFs.